Maxwell's demon as a dynamical model

G. M. Zaslavsky and M. Edelman
Courant Institute of Mathematical Sciences, New York University, 251 Mercer Street, New York, New York 10012
and Department of Physics, New York University, 2-4 Washington Place, New York, New York 10003
(Received 21 January 1997; revised manuscript received 5 May 1997)

We consider a model of a billiard-type system, which consists of two chambers connected through a hole. One chamber has a circle-shaped scatterer inside (Sinai billiard with infinite horizon), and the other one has a Cassini oval with a concave border. The phase space of the Cassini billiard contains islands, and its parameters are taken in such a way as to produce a self-similar island hierarchy. Poincaré recurrences to the left and to the right chambers are considered. It is shown that the corresponding distribution function does not reach ''equipartition'' even during the time 10^{10}. The explanation is based on the existence of singularities in the phase space, which induces anomalous kinetics. The analogy to the Maxwell's Demon model is discussed.
[S1063-651X(97)08811-9]

PACS number(s): 05.45.+b

I. INTRODUCTION

In 1871, Maxwell proposed a conceptual device that could make molecules select one of two equal chambers connected through a hole. This device (Demon), located at the hole, should work against the thermodynamic law, which causes the gas of molecules in two contacting volumes to be in equilibrium. We can recommend an excellent collection of the principal publications on the Maxwell's Demon problem [1] accompanied by a comprehensive editorial review. The problem, however, leaves an ambiguity in regard to its precise definition as it involves a nonphysical element as a part of the full construction. In contemporary physics, this element is specified, which helps the Maxwell's Demon to acquire a different, realistic visualization:

(i) The Demon can be considered as a device that is able to work with information and transfer the information into action (thinking device).
(ii) The Demon is a measuring device, and its actions depend on the results of the measurement.

Both concepts give rise to rich physical discussions on the possibilities of computing devices, irreversibility of computations, natural limitations of the measurement process, role of quantum effects, and the quantum uncertainty.

In Ref. [2], we proposed a direction for studying the Maxwell's Demon (MD) problem, based on its complete dynamical formulation and avoiding any types of elements that cannot be formulated as equations of motion. Dynamical chaos makes it possible to formulate a new version of the MD problem. In his original publication, Maxwell wrote that in statistical consideration ''. . . we are compelled to adopt . . . the statistical method of calculations and to abandon the strict dynamical method in which we follow every motion by calculus.'' Hence we are just going to follow strict dynamics.

The general idea of the proposed approach to the problem can be fairly simply formulated. Consider two separate dynamical systems with such mixing properties of the trajectories so that a statistical equilibrium can be achieved in each of the systems. Let us make a weak contact between the systems, which brings the coupled subsystems to a new equilibrium state. One may ask the question: Does the new equilibrium for each subsystem correspond to what we commonly define as thermodynamical equilibrium (equal pressures, temperatures, etc.)?

In [2], a prototype of the dynamical model was introduced, consisting of two billiardlike systems with mixing motion inside each and with the contact of billiards through a hole. A point particle is bouncing inside the billiards with absolutely elastic reflections from the billiards' walls. As both billiards have mixing properties, a stationary distribution function is expected. It can be a probability measure to find a particle in one or another part of the system in the infinite time limit. For the ergodic motion the infinite time limit can be replaced by an ensemble average in the phase space of a system. Can the equilibrium in the described billiardlike system be of the same kind as the one we usually call thermodynamic equilibrium? Or, in other words, can the Hamiltonian chaotic dynamics explain, in principle, the origin of the thermodynamics law, or do we need some additional restrictions? In this article, we will show a negative answer to this question, considering an appropriate ''design'' of the billiardlike system with chaotic dynamics.

Actually, the main goal of this discussion is to determine what kind of random process corresponds to the dynamical chaotic motion. It is well known that this problem is quite complicated. For the Hamiltonian systems of general type, the motion is not ergodic. To obtain a domain or ergodic motion, one needs to extract, from the entire phase space, a (multi) fractal set of islands with regular motion. The properties of the rest of the phase space, call *stochastic sea*, are almost as poorly understood as those of islands' boundaries. This part of the phase space is nonuniform. It is filled by another kind of fractal object, *cantori*, which have zero measure and strongly influence the transport of particles [3], probably creating a ''stickiness'' of the islands' boundaries [4].

The situation with islands occur not simply because they can appear or disappear [5,6], depending on the values of control parameters. It seems that there is no unique scenario to explain the stickiness of the boundary of islands. One of

the possible scenarios is related to the existence of an islands-around-islands structure of the boundary. The origin of such a topology of islands was described in [7] and, from another viewpoint, in [5]. The type of an island set in the boundary layer depends on the value of a control parameter. It was shown in [6] (for example) that for some special values of the perturbation parameter for the standard map and web map, there exists an exact self-similar set of islands around islands that generates enormously long flights. Any flight means a fairly long and almost regular part of a trajectory. Usually, these flights correspond to the trapping of trajectories in some boundary layer near the islands. The smaller the island, the longer (generally) the flight.

The existence of islands and flights around them leads to a nonuniformity of the distribution function of particles in the stochastic sea. It was found in [8] that spikes in the distribution function due to the stickiness can be considered as transient phenomena because after 10^{10} iterations of the standard map the spikes dissolve. A special value of the control parameter was considered in [8], which corresponds to the so-called golden last rotational invariant circle. In this paper we consider another model, connected billiards, using an even larger number of iterations (10^{10}–10^{11}), which generates enormously long flights due to a special choice of the control parameter. Our data show that at least for the connected billiard the time 10^{10}–10^{11} is insufficient to decide whether the nonuniformity of the phase space is transient, but even without complete data, it is clear that the transient time can be so huge as to necessitate the introduction of a new kind of kinetics describing the motion with flights [6,9,10]. We have to admit that the existence of a powerlike tail in the correlation function does not follow directly from the existence of an infinite island's hierarchy. This point is still unclear for typical dynamical systems. One can consider it as a problem for chaotic systems to understand how the ''scarring'' of the phase space can influence the global transport properties. The dissolving of the spikes for a fairly large time, obtained in [8], can be treated as an interesting observation to be taken into account.

Crucial to the understanding of chaotic dynamics is the notion of fractal time described in [11,12] and applied to some dynamical systems in [10,6]. Following [6,13,14], one can use the fractal time concept to describe Poincaré recurrences for a system with Hamiltonian chaotic dynamics. The distribution function of the recurrence time has a powerlike tail, which means an enormously long time of convergence for the ergodic theorem and divergence of moments after a certain point. All these anomalies can be expressed in a compact way: typical Hamiltonian chaotic dynamics does not follow a typical kinetics and cannot be described by the regular thermodynamics. Nevertheless, this statement does not exclude the possibility of ''normal'' kinetics and thermodynamics for restricted or very large time scale and for special values of the parameter.

In this paper, we present an example that demonstrates the absence of the thermodynamic-type equilibrium within the time corresponding to about 10^{10} iterations, using billiardlike systems with chaotic dynamics.

II. DESCRIPTION OF THE MODEL

Billiards can be considered as one of the most attractive types of dynamical models to study ergodic and mixing properties of Hamiltonian systems. A particle in a billiard with absolutely elastic collisions was used for the analysis of the origin of statistical laws [15–17]. Here we would like to go further and use billiard-type systems to study the origin of thermodynamical laws. In particular, we will consider the appearance of equilibrium distributions and their moments.

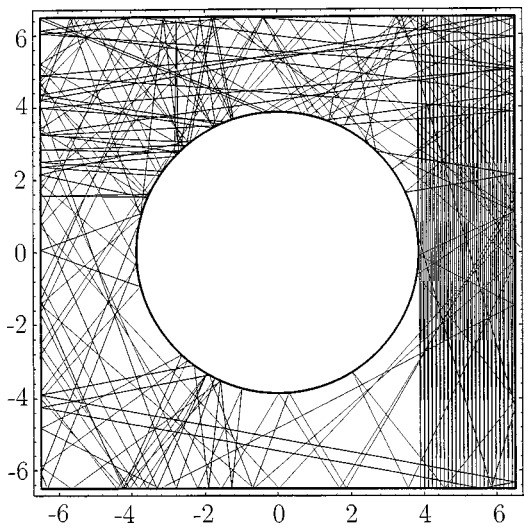

FIG. 1. Example of a trajectory with a very long flight in the Sinai billiard: box 13×13; radius 3.86.

Our system will consist of two subsystems, each being a kind of a billiard. One subsystem is the so-called Sinai billiard (Fig. 1). It has a convex scatterer (circle) inside a square box. Trajectories can be displayed in the four-dimensional phase space. The Sinai billiard can be transferred in the so-called Lorentz gas if we consider a double-periodical continuation of the set of scatterers, eliminating the walls of the billiard.

The second subsystem will be called the Cassini billiard in which the scatterer has the shape of Cassini's oval:

$$(x^2+y^2)^2-2c^2(x^2-y^2)-(a^4-c^4)=0. \qquad (2.1)$$

The shape of the oval is sensitive to the parameters a, c and can have concave and convex parts (see the example in Fig. 2). The phase space of the Cassini billiard is much more complicated that of the Sinai billiard, since it allows a nonergodic motion in a finite measure domain due to the presence of islands in the phase space. One can also consider an analog of the Lorentz gas if the double-periodic continuation of the scatterers is made.

Considering a bounded billiard with any type of scatterer, we expect a stationary distribution function after a ''while.'' In fact, this statement needs a serious comment, which will be made below. Some of the moments of the stationary distribution function play the same role as thermodynamical characteristics of the system. Now let us introduce a model to be studied. Consider Sinai and Cassini billiards contacting through a small hole in the dividing wall as shown in Fig. 3 (C-S billiard). After a ''while,'' we can expect a stationary distribution for the C-S billiard. Also, we can define some distribution functions for the left and right halves of the C-S system, normalize these distributions, and calculate left and right moments of the distributions. The question is: Are the left and right moments the same? In the case of a negative

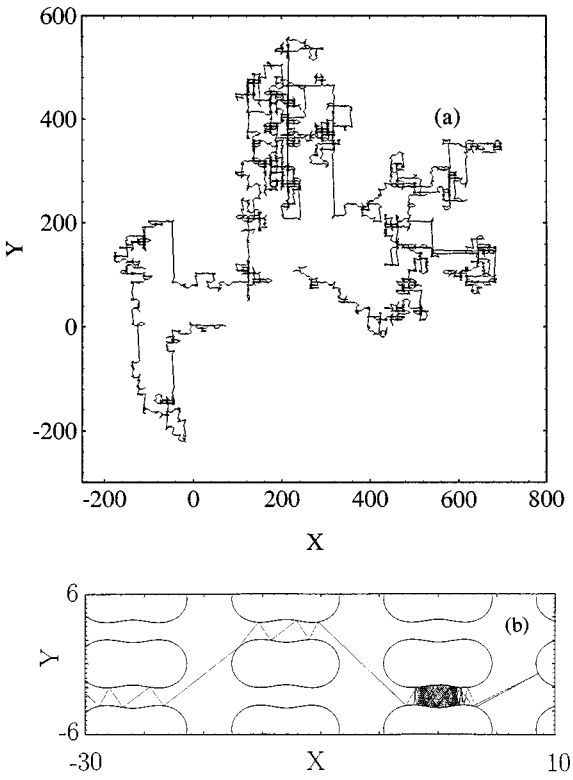

FIG. 2. Example of a trajectory with many long flights (a) and a long trapping (b) in the Cassini billiard with the parameters $a=3.496\,0393$, $c=3$.

answer there is reason to interpret the results as an absence of the thermodynamic-type equilibrium between left and right subsystems. We can also assume that the nonthermodynamic-type equilibrium corresponds to a metastable or transient situation with an arbitrary long span.

III. POINCARÉ RECURRENCES AND THE TIME-SCALE PROPERTIES

Distribution of the Poincaré recurrents will play a crucial role in our consideration. Consider a fairly small domain $\Delta\Gamma$ in the phase space of a system and a set of time instants $\{t_j\}=t_1,t_2\ldots$ of a trajectory's consequent exits from $\Delta\Gamma$. A set of intervals $\{\tau_j\}=\{t_j-t_{j-1}\}$ is called recurrence times, and $P(\tau;\Delta\Gamma)$ is their density probability distribution function for the domain $\Delta\Gamma$. We can exclude $\Delta\Gamma$, introducing a new density,

$$P(\tau)=\lim_{\Delta\Gamma\to 0}\frac{1}{\Delta\Gamma}P(\tau;\Delta\Gamma) \tag{3.1}$$

and assuming the existence of the limit (3.1). The probability density $P(\tau)$ to have the length of a recurrence cycle within the interval $(\tau,\tau+d\tau)$ is normalized,

$$\int_0^\infty P(\tau)d\tau=1, \tag{3.2}$$

and its moments can be introduced in a regular way:

$$\langle\tau^n\rangle=\int_0^\infty \tau^n P(\tau)d\tau. \tag{3.3}$$

For the case of dynamical chaos with fairly good mixing properties one can expect a Poissonian law:

$$P(\tau)=\frac{1}{\langle\tau\rangle}\exp(-\tau/\langle\tau\rangle). \tag{3.4}$$

(See [18–22]. More discussions of this topic are in [23].) Nevertheless it is now clear that the nonergodicity of the full phase space induces a powerlike tail of the distribution $P(\tau)$. This phenomenon was observed for different systems with continuous time [19,22], for billiards [24–26], and for the web map and standard map [6,27–30]. There is some evidence that the powerlike asymptotic dependence

$$P(\tau)\sim\tau^{-\gamma} \tag{3.5}$$

correlates with the presence of anomalous transport [22,28,29]. The phenomena of anomalous (non-Gaussian) transport for billiards was studied in numerous publications (see, for example, [31–34, 24–26]). For different types of systems, the anomalous kinetics was explained by the presence of so-called Lévy flights (see a review [9] on ''strange kinetics'').

Surprisingly, a general restriction can be imposed on the exponent γ. It was proved in [35] that for the compact phase space and ergodic motion with nonzero measure, the mean recurrence time $\langle\tau\rangle$ is finite

$$\langle\tau\rangle<\infty. \tag{3.6}$$

Moreover,

$$\langle\tau\rangle=\Gamma_0/\Delta\Gamma, \tag{3.7}$$

where Γ_0 is an admissible volume (usually it is put $\Gamma_0=1$) and $\Delta\Gamma$ is a volume of the domain of observation. This result was reformulated in [36] in a form that permits to conclude [37]:

$$\gamma>2. \tag{3.8}$$

The condition (3.8) is equivalent to Eqs. (3.6) and (3.7). In particular, for the Sinai billiard of the type shown in Fig. 1, which corresponds to the so-called Lorentz gas with infinite horizon, it was found [24]

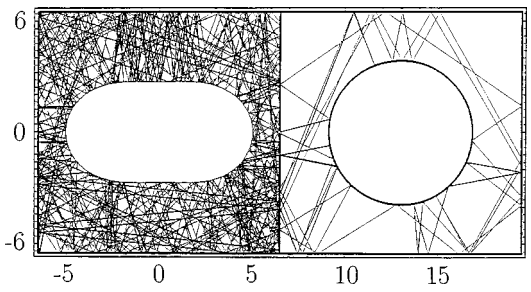

FIG. 3. Example of a trajectory in the Cassini and Sinai billiards contacting through a hole. Parameters of the Sinai billiard are the same as in Fig. 1 and for the Cassini billiard: $a=4.030\,952$, $c=3$. The hole size is 0.2.

$$\gamma = 3 \tag{3.9}$$

The connection between the properties of the anomalous kinetics and Poincaré recurrences led to a stronger result that was derived for the web map and standard map [6,28]:

$$\gamma = 2 + \mu, \tag{3.10}$$

where μ is an exponent of the anomalous kinetics

$$\langle R^{2m} \rangle \sim t^{m\mu} \quad (t \to \infty). \tag{3.11}$$

R is a particle displacement during the time interval t in the phase space, and m is an integer. The expression (3.10) was obtained by applying the renormalization-group method to the boundary layer of an accelerator mode island for which the subislands form a self-similar structure. This situation occurs for some special values of the control parameter. The result (3.10) can be used for a general situation when the island structure is self-similar and the space-time renormalization can be applied. Specific conditions are discussed in more detail in [6]. For the Sinai billiard, a hierarchical islands structure does not exist. Nevertheless, for the case of infinite horizon, $\mu = 1$ up to a logarithmic term, and there is no contradiction between Eqs. (3.9) and (3.10). A more complicated case of the Cassini billiard will be discussed below. A finite value of γ makes moments $\langle \tau^n \rangle$ infinite. For $0 < \mu < 2$, the moments of the distribution function of Poincaré cycles are infinite, starting from $n = 2$ in the subdiffusion case ($0 < \mu < 1$) and from $n = 3$ in the superdiffusion case ($1 < \mu < 2$).

To complete this section, we will determine a connection between $P(\tau)$, given by Eq. (3.5), and the escape probability. Consider a small domain $\Delta\Gamma$ in the area of a singular zone. We assume the existence of such a zone (or zones), which are responsible for the anomalous properties of kinetics (see more about the zones in [6]). Let $\psi(\tau)d\tau$ be the probability of a particle to escape from the domain $\Delta\Gamma$ in a time instant τ within the interval $(\tau, \tau + d\tau)$. The probability to escape from $\Delta\Gamma$ during a time $\leqslant t$ is

$$\Psi_e(t) = \int_0^t \psi(\tau) d\tau \tag{3.12}$$

and the survival probability is

$$\Psi_s(t) = 1 - \Psi_e(t) = \int_t^\infty \psi(\tau) d\tau, \tag{3.13}$$

where the following boundary condition have been used:

$$\Psi_e(\infty) = 1, \quad \Psi_s(\infty) = 0. \tag{3.14}$$

Let us assume the existence of a powerlike tail for the escape probability density,

$$\psi(\tau) \sim \tau^{-1-\beta} \quad (\tau \to \infty), \tag{3.15}$$

with a characteristic exponent β and assume that there exists a single zone with a single characteristic exponent β. Then Eq. (3.15) defines the longest escapes from the singular zone, and the same exponent should be taken for the Poincaré recurrences distribution (3.5). It was suggested in [6] that long-time recurrences occur after the corresponding orbits have entered and then escape from a singular zone. This provides a possibility to put $\gamma = 1 + \beta$, or, after comparing Eq. (3.15) to Eqs. (3.5) and (3.10),

$$\gamma = 1 + \beta = 2 + \mu, \quad \beta = 1 + \mu. \tag{3.16}$$

We will discuss the values of γ, β, μ in more detail in the following sections.

From the results obtained above, it follows that the first moment $\langle \tau \rangle$ of the Poincaré cycle distribution is a very rough characteristic of the dynamics and the higher moments should be used to distinguish between the systems with singular zones in their phase space. Such a difference in regard to singular zones permits one to speculate on the subject of the Maxwell's Demon [2]. This consideration will be continued in this paper.

IV. CASSINI BILLIARD

In this section, a numerical simulation of some properties for the Cassini billiard (Fig. 2) is presented. The inner scatterer is a Cassini's oval (2.1). We can create different regimes of scattering by changing parameters a and c. The phase space of the billiard belongs to a ''regular'' case; i.e., there are islands in the stochastic sea. The Poincaré section for trajectories consists of points (x, v_x) or $(x, \phi)$where x is the intersection coordinate of a trajectory and the bottom side of the billiard, and $v_x = \sin\phi$, i.e., ϕ is the angle between $\mathbf{v}$ and a normal to the x axis. The invariant Lebesgue measure (stationary distribution function) is nonzero on the (x, v_x) plane, except for the islands and zero-measure line segments that correspond to the bouncing trajectories with $v_x = 0, \pm 1$ ($\phi = 0, \pm \pi/2$).

An example of the phase plane with islands and stochastic sea is shown in Fig. 4(a). The set of islands belongs to the fourth order resonance and dark strips around some islands correspond to the islands' stickiness; i.e., the trajectory spends a longer time rotating around the island near its boundary. The stickiness observed in Fig. 4(a) corresponds to a ballistic mode regime. For the infinite phase space with periodically continued scatterers like those in Fig. 2(a), the ballistic mode corresponds to very long segments of a trajectory that bounces between two (or more) arrays of scatterers. The same trajectory as in Fig. 4(a) is plotted in Fig. 4(b) in infinite coordinate space, and it reveals many flights that correspond to the trajectory being stuck at the boundary of different islands.

The occurrence of ballistic modes is a general property of Hamiltonian dynamics (see discussions in [6,28]). They can be easily observed for some special values of parameters when an ordered set of islands is generated. For the case in Fig. 4, the values are $a = 4.030952$ and $c = 3$, and the corresponding alternating hierarchy of subislands 4-8-4-8-... is shown in Fig. 5. It was mentioned in [5,6,29] that an ordered sequence of islands possesses scaling properties of the islands' space-time characteristics. However, only one value of the proliferation coefficient q was considered, so the number of islands of different generations followed the sequence $q, q^2, q^3, \ldots$. In the case shown in Fig. 4, two values of the proliferation coefficient, $q = 4$ and $q = 8$, alternate.

Table I displays values of proliferation coefficient q_k for

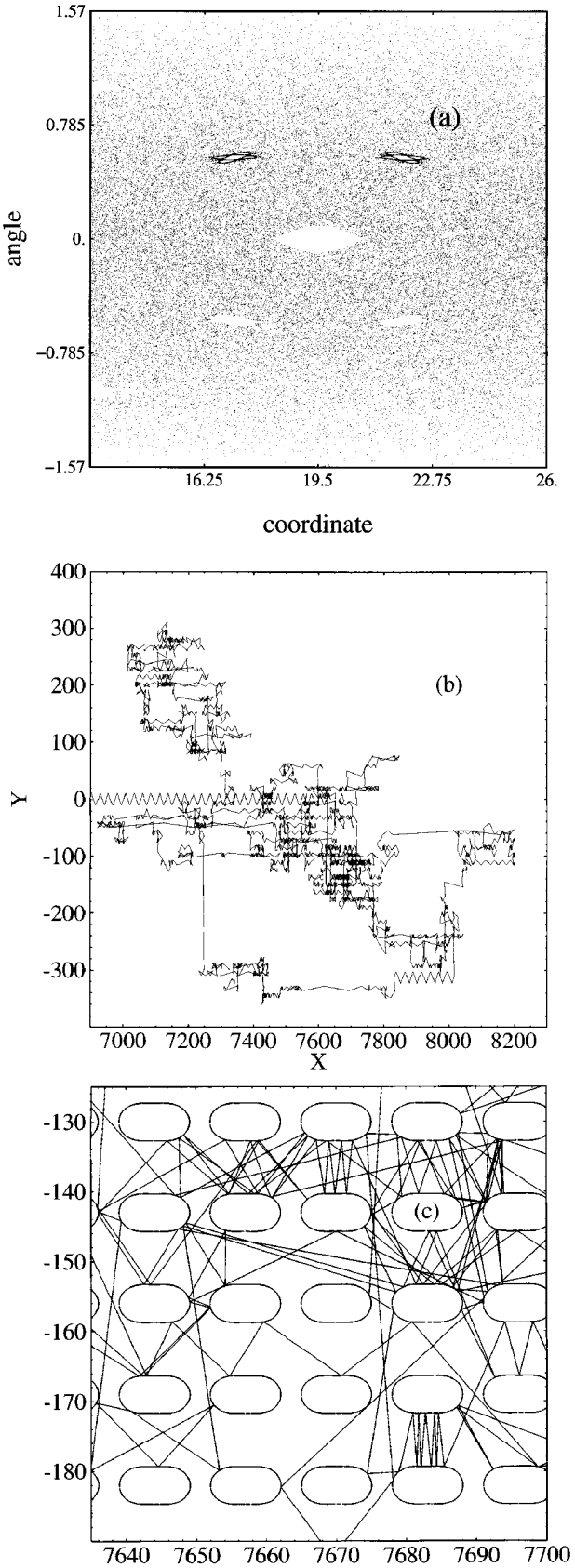

FIG. 4. A sticky trajectory with different flights for the Cassini billiard with parameters $a=4.030\,9525$, $c=3$, box 13×13. (a) Poincaré map in the space (x,ϕ) with islands; angle ϕ is in radians (b) the same trajectory in the coordinate space; (c) element of the same trajectory, which demonstrates the origin of bouncing flights.

the kth generation, period T_k of the last invariant curve inside an island of kth generation, area ΔS_k of an island of kth generation, and the area

$$\delta S_k = q_k \Delta S_k \tag{4.1}$$

of all islands of kth generation. In accordance with [10], two scaling parameters are introduced in order to describe a self-similarity of the islands' hierarchy:

$$\lambda_S^{(k)} = \delta S_k / \delta S_{k-1}, \qquad \lambda_T^{(k)} = T_k / T_{k-1}. \tag{4.2}$$

For a constant value of $q_k = q(\forall k \geqslant 1)$, the simulation confirms the existence of constant values of scaling parameters

$$\lambda_S^{(k)} = \lambda_S, \quad \lambda_T^{(k)} = \lambda_T \quad (\forall k \geqslant 1) \tag{4.3}$$

for the web map and standard map [6,28,29]. For the case in Fig. 5, we have a new situation with two values of $\lambda_S^{(1,2)}$, $\lambda_T^{(1,2)}$ that can be found from Table I:

$$\lambda_T^{(1)} \sim 7.45, \quad \lambda_T^{(2)} \sim 4.16, \qquad \lambda_S^{(1)} \sim 0.0174, \quad \lambda_S^{(2)} \sim 0.21, \tag{4.4}$$

where the mean values are taken, and we skip $\delta S_1 / \delta S_0$, which does not correspond to the set ($q_0 \neq 8$).

A transport exponent μ was introduced in [10,6] [compare to Eq. (3.10)] using the equation

$$\langle R^{2m} \rangle \sim t^{m\mu} \quad (t \to \infty), \tag{4.5}$$

with integer m. For special cases when the anomalous transport is caused by the stickiness near a self-similar hierarchy of islands, the following explicit expression was derived:

$$\mu = |\ln \lambda_S| / \ln \lambda_T \tag{4.6}$$

for the superdiffusive kinetics due to the ballistic (accelerator) modes. For the case of periodic sequences $q_0, \ldots, q_m, q_0, \ldots, q_m, \ldots$ the formula (4.6) can be easily generalized. The effective scaling for the islands area is

$$\lambda_S = [\lambda_S^{(1)} \ldots \lambda_S^{(m)}]^{1/m} \tag{4.7}$$

and a similar expression is for scaling of periods:

$$\lambda_T = [\lambda_T^{(1)} \ldots \lambda_T^{(m)}]^{1/m}. \tag{4.8}$$

Substitution of Eqs. (4.7) and (4.8) into (4.6) gives

$$\mu = \sum_{j=1}^{m} |\ln \lambda_S^{(j)}| / \sum_{j=1}^{m} \ln \lambda_T^{(j)} \tag{4.9}$$

(for more details see [14]). Then for the case (4.4) when $m=2$, we have

$$\mu = (|\ln \lambda_S^{(1)}| + |\ln \lambda_S^{(2)}|) / (\ln \lambda_T^{(1)} + \ln \lambda_T^{(2)}). \tag{4.10}$$

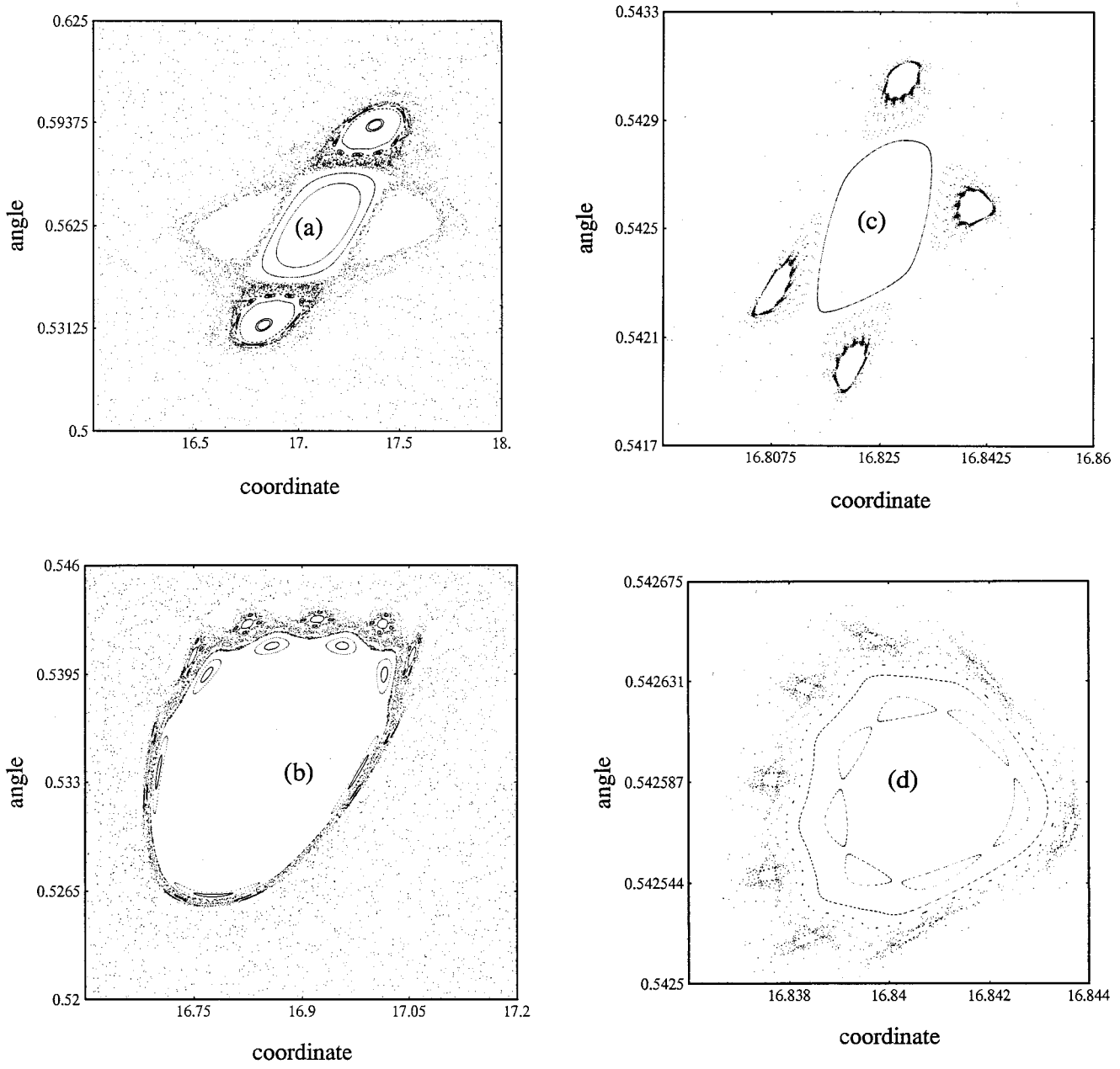

FIG. 5. Four consequent hierarchies of islands for the case in Fig. 4, which represent the sequence 4(a)-8(b)-4(c)-8(d). The angle is in radians.

The diffusion for Cassini billiards was simulated for the same parameters as in Figs. 4 and 5 and for the moments $\langle R^{2m}\rangle$ with $m=1,2,3,4$. The observation time was 10^6 and the averaging was performed over 187 500 initial conditions. The results demonstrated in Fig. 6 give $\mu=1.55\pm0.07$, which is in good agreement with the value $\mu=1.59$ obtained from Table I and expression (4.10). The second moment $\langle R^2\rangle$ gives the largest deviation from the mean value $\mu=1.55$.

The above example of trajectories with flights can be well understood. It makes this case convenient for considering the model of two contacted billiards as shown in Fig. 3. We will

TABLE I. Parameters of the islands hierarchy in the sequence 2-4-8-4-8.

k	q_k	T_k	T_k/T_{k-1}	ΔS_k	$\Delta S_k/\Delta S_{k-1}$	δS_k	$\delta S_k/\delta S_{k-1}$
0	2	16.36		1.47×10^{-2}		2.94×10^{-2}	
1	4	118	7.21	3.96×10^{-3}	2.69×10^{-2}	3.17×10^{-2}	1.08
2	8	508.9	4.31	8.53×10^{-6}	2.15×10^{-3}	5.46×10^{-4}	0.017
3	4	3910	7.69	4.4×10^{-7}	5.2×10^{-2}	1.1×10^{-4}	0.21
4	8	15740	4.02	0.96×10^{-10}	2.2×10^{-3}	2.0×10^{-6}	0.018

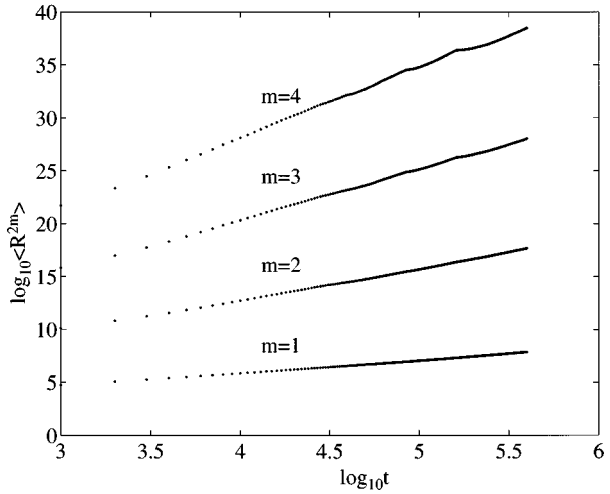

FIG. 6. Log_{10}-log_{10} plot of the moments of displacement as function of time for Cassini billiard. All parameters are the same as in Fig. 4. The number of trajectories is 187 500.

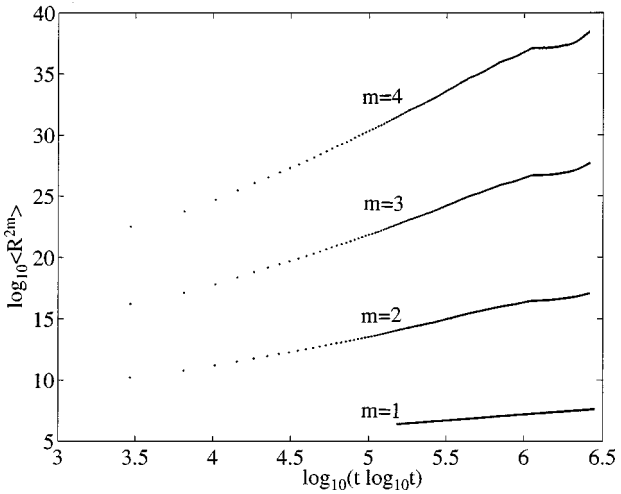

FIG. 7. Log_{10}-log_{10} plot of the moments of displacement as a function of time for Sinai billiard. Parameters of the billiard are the same as in Fig. 1; the number of trajectories is 187 500.

discuss the Cassini billiard properties in more detail in Secs. VI and VIII.

V. SINAI BILLIARD

We have already discussed some properties of the Sinai billiard in Secs. II and III. In this section, we consider only one specific property of the Sinai billiard—the moments of displacements $\langle R^{2m}\rangle$ as a function of time (see Fig. 1). The periodic extension of Fig. 1 in x and y directions transforms the billiard model into the periodic Lorentz gas with an infinite horizon; i.e., arbitrary long flights are available for a particle moving between circular scatterers.

Qualitative arguments were proposed for the velocity correlation asymptotic [34,26]

$$\langle \mathbf{v}(0)\mathbf{v}(t)\rangle \sim \mathrm{const}/t, \tag{5.1}$$

which leads for the mean square displacement

$$\langle R^2\rangle \sim \mathrm{const}\times t\ \ln t. \tag{5.2}$$

It is difficult to obtain a sufficiently accurate simulation to confirm the presence of the logarithmic multiplier in Eq. (5.2). Up to this factor, the result (5.2) was rederived and simulated in a number of articles [24–26,31–34]. It was proposed in [24] that ''For any periodic configuration of scatterers with an infinite horizon the limit in distribution

$$\eta = \lim_{t\to\infty} \frac{\mathbf{x}(t)-\mathbf{x}(0)}{(t\ \ln t)^{1/2}} \tag{5.3}$$

exists and η is a Gaussian random variable.''

In fact, there is no rigorous proof of either Eq. (5.3) or (5.2). Our simulation of the periodic Lorentz gas model with infinite horizon is consistent with Eq. (5.2) and not consistent with Eq. (5.3). The simulation was performed for the time 10^6 and 187 500 initial conditions. The result is displayed in Fig. 7. With fairly high accuracy, we can express the result in the form

$$\langle R^{2m}\rangle \sim (t\ \ln t)(t\ \ln t)^{1.5(m-1)}, \tag{5.4}$$

which is not of the Gaussian type and can be related to a strongly anomalous transport. Although we cannot interpret the result (5.4), it is clear that it can be caused by the only kind of singularity in the phase space of the model, i.e., by zero measure line segments responsible for the free infinitely bouncing trajectories that do not touch scatterers or touch them periodically.

VI. CONTACTED CASSINI AND SINAI BILLIARDS

Now we shall consider a model in Fig. 3, which corresponds to contacted Cassini (left chamber) and Sinai (right chamber) billiards through a hole in their common side. Consider a trajectory and count time instants $\{t_j^{(C)}\}$, $\{t_j^{(S)}\}$ when the particle leaves C (Cassini chamber) or S (Sinai chamber) correspondingly. Then the sequences

$$\begin{aligned} \{\tau_{j+1}^{(C)}\} &= \{t_{j+1}^{(C)} - t_j^{(S)}\}, \\ \{\tau_{j+1}^{(S)}\} &= \{t_{j+1}^{(S)} - t_j^{(C)}\}, \end{aligned} \tag{6.1}$$

can be related to the time intervals that a particle stays in C, or in S when the systems are contacted. One can also say that the sequences (6.1) are recurrence times to the domain Δ covered by the hole, and $\{\tau_j^{(C)}\}$, $\{\tau_j^{(S)}\}$ are sets of the left or right recurrences correspondingly. In the case when there is no hole, we should replace $t_j^{(S)}$ by $t_j^{(C)}$ and $t_j^{(C)}$ by $t_j^{(S)}$ in Eq. (6.1) and simply get Poincaré recurrences for C and S billiards independently.

The corresponding simulation was performed for a single trajectory over $t \cong 10^{10}-10^{11}$, which corresponds to about 10^9-10^{10} crossings of a billiard (chamber). The size of the hole was 0.2 while the size of a side was 13. The phase volumes of both billiards were equal, and the accuracy was up to 10^{-3}.

The results for the probability distribution densities $P(t,\Delta)$ of Poincaré recurrences for the isolated C and S billiards are shown in Fig. 8. The probability follows the

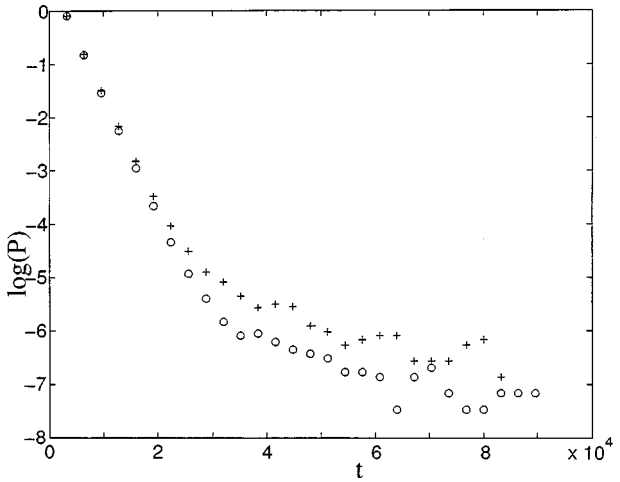

FIG. 8. Distribution of the Poincaré recurrences for the Sinai (S) billiard (circles) and Cassini (C) billiard (crosses). Parameters are the same as in Figs. 1 and 4. Computing time 10^{11} for S and 1.5×10^{10} for C.

Poissonian law (3.4) until $t_0\sim2\times10^4$ with the same mean time $\langle\tau\rangle$ in agreement with the Kac result (3.6) and (3.7). The value of t_0 corresponds to the chosen domain Δ. We made sure that the behavior obtained in Fig. 8 did not depend on the size and location of the domain Δ although the crossover time t_0 did.

For $t>2\times10^4$, the deviations from the Poissonian law begin to occur, and long tails can be observed. The difference between these two distributions is evident and can be expressed more clearly using the high moments of $P(t,\Delta)$:

$$\langle\tau^m\rangle=\int_0^{t_{\max}}t^mP(t,\Delta)dt \tag{6.2}$$

[compare Eq. (6.2) to Eq. (3.3)]. Figure 9 presents the corresponding moments up to $m=10$ normalized to $\langle t\rangle$ for C and S with $t_{\max}\sim10^{11}$. Starting from $m=5$, the difference approaches the value of about one order of magnitude. Nevertheless, important for us is not only the difference in the recurrence distribution functions and its high moments, but also the existence of a difference for the first moments, which are

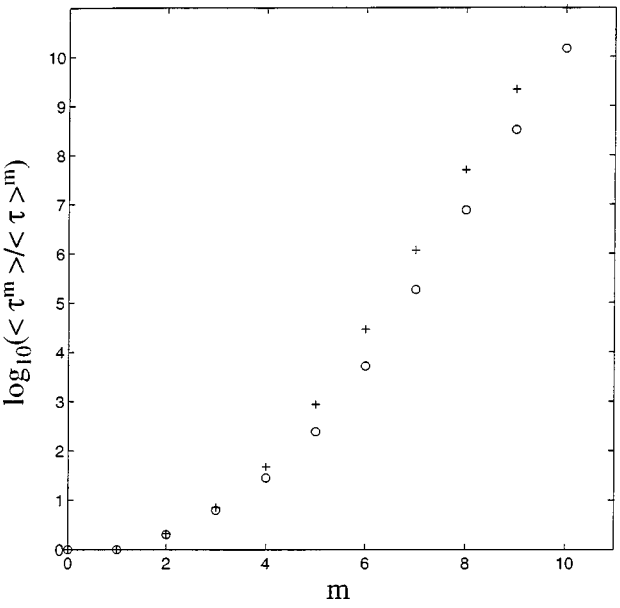

FIG. 9. Moments of the distribution of Poincaré recurrences that are shown in Fig. 8, with the same parameters and the same notations.

$$\langle t^{(C)}\rangle=1.97\times10^3,\quad \langle t^{(S)}\rangle=1.92\times10^3,$$
$$\langle\Delta t^{(C\text{-}S)}\rangle=\langle t^{(C)}\rangle-\langle t^{(S)}\rangle=0.05\times10^3. \tag{6.3}$$

This is consistent with the level of resolution of our computations, i.e., $\langle\Delta t^{(C\text{-}S)}\rangle$ is much larger than the value $10^{-3}\langle t^{(C\text{-}S)}\rangle$, which is the accuracy of the phase volume evaluation. The difference $\langle\Delta t^{(C\text{-}S)}\rangle\neq0$ occurs because the distribution of recurrences is still not stationary despite a very long computation time, and the tail influence is still sensitive to the value $\langle t\rangle$.

To get the exponent γ of the power tail in the recurrences distribution

$$P(t)\sim\text{const}/t^\gamma \tag{6.4}$$

[compare to Eq. (3.5)], we performed a longer computation with $t_{\max}=2\times10^{11}$ (Fig. 10) and obtained $\gamma=3.02$ for the Sinai billiard, which was in agreement with the theoretical prediction $\gamma=3$ [24]. The dispersion of points in Fig. 10(a) is very small, which allows us to claim that the exponent γ is very close to the predicted one.

The origin of the value $\gamma=3$ is the presence of nonscattered bouncing trajectories and the corresponding singularity of the phase space. The same kind of singularity exists independently on the shape of the surface of a scatterer and one can expect a universality of the low $\gamma=3$. In fact, it was observed [Fig. 10(b)] that for the Cassini billiard with the same parameters as in Fig. 8 $\gamma=3.15$, which is consistent with the above comment. A small excess of γ can be explained by the influence of the ballistic mode. If no other singularities exist, the flights due to the islands hierarchy in Fig. 4 lead to [6]

$$\gamma=2+\mu, \tag{6.5}$$

i.e., $\gamma\cong3.6$, which is larger than $\gamma=3$. That means that the tail $1/\tau^{3.6}$ in the distribution (6.4) decays faster than the ''regular'' tail $1/\tau^3$.

Now we shall consider the contacted two chambers containing a Cassini oval and a circle as shown in Fig. 3. The size of the hole is 0.2. In order to increase its anomalous kinetics level, we keep the same parameters for the Cassini oval as in Fig. 4. Also, we adjust the Sinai billiard circle as in Fig. 1 in order to have equal phase volumes for both chambers. The corresponding distributions $P_C(t)$ and $P_S(t)$ of the times that a particle stays in C or in S, defined in Eq. (6.1) for the left (Cassini billiard) and right (Sinai billiard) chambers, are presented in Fig. 11. We also display the corresponding moments $\langle t_C^m\rangle$, $\langle t_S^m\rangle$of the distributions $P_C(t)$, $P_S(t)$ in Fig. 12. The absolute differences of moments for the cases with and without a contact between the chambers can be found in Table II. All these results were obtained for 37 trajectories of time length 1.6×10^{10} each.

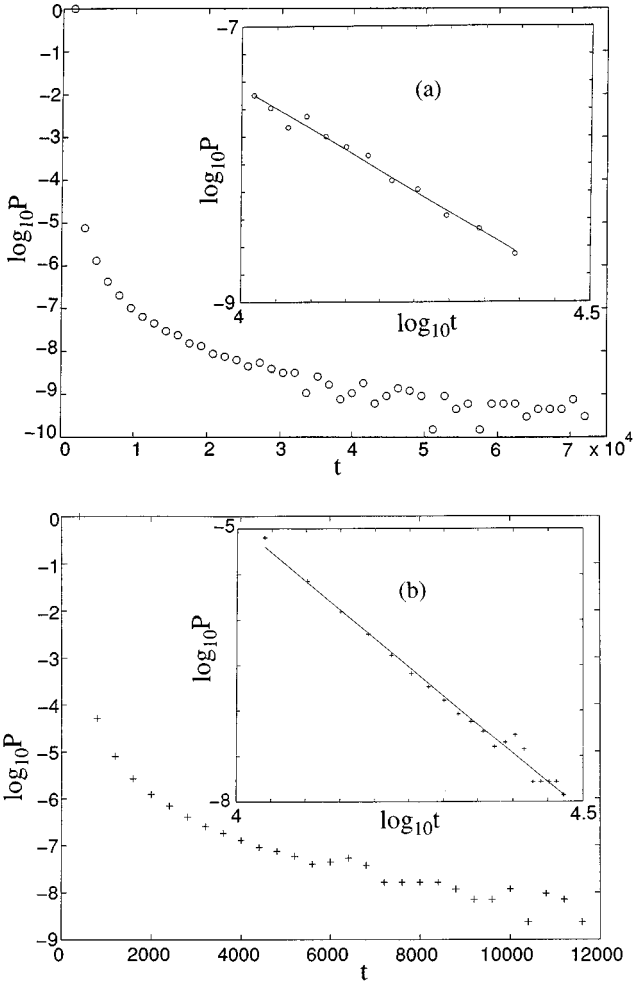

FIG. 10. Tails of the distribution of Poincaré recurrences shown in Fig. 8 for Sinai (a) and Cassini (b) billiards. Inner boxes display log-log plot and approximate a straight line. The slopes are 3.02 for S and 3.15 for C.

The results presented in Figs. 11 and 12 and in Table II lead to the following conclusion. There is no equilibrium in the usual thermodynamic sense, at least during the observation time $t_{\max} \sim 10^{10}$, or $\sim 10^9$ characteristic periods. It was

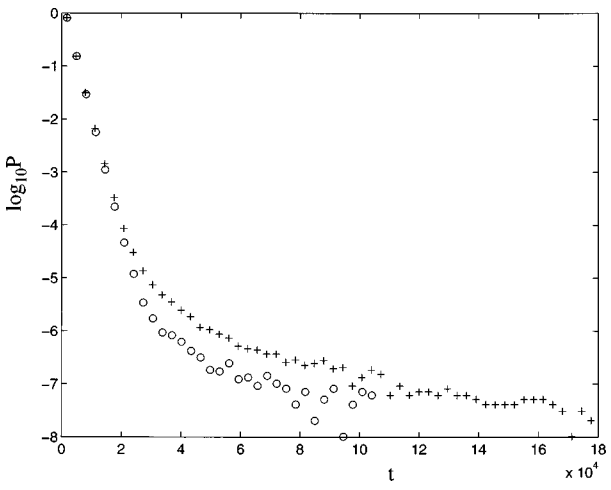

FIG. 11. The same as in Fig. 8 but with a connection of C-S billiards. The hole in 0.2. Number of trajectories is 37. Computing time is 1.16×10^{10} for each trajectory.

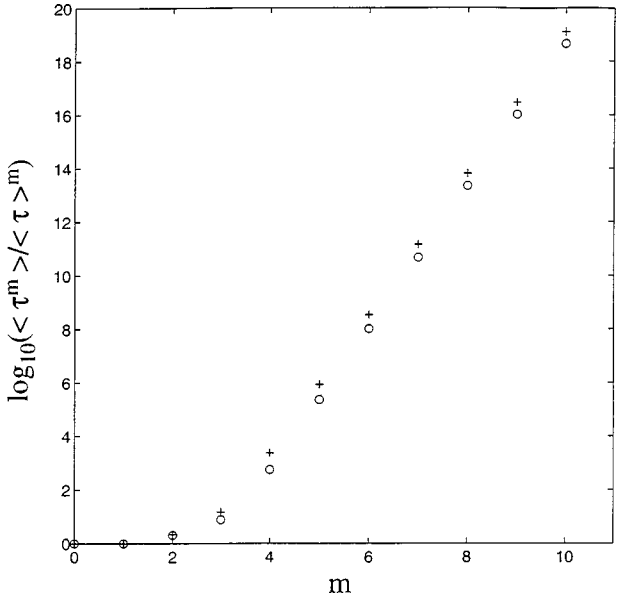

FIG. 12. The same as in Fig. 9 but with a connection of C-S billiards. Parameters are the same as in Fig. 11.

mentioned above that the distributions $P_C(t)$, $P_S(t)$ are actually the Poincaré cycle distributions and they should not depend on the location of a volume $\Delta\Gamma$ of the observation in the case of macroscopic equilibrium. In this sense the described situation does not correspond to an equilibrium, since the distribution functions and their moments are significantly different for both chambers. One can also manifest the absence of a fast relaxation process, which can lead to an equilibrium in a finite time.

VII. COMMENTS ON THE NUMERICAL SIMULATIONS

Trajectories were mapped using standard double precision computations. The point of a trajectory intersection with Cassini's oval was obtained with a precision higher than 10^{-11}. The phase volume of the Cassini billiard was obtained using the Monte Carlo method. The phase volume with islands was partitioned into 250^3 cells and the trajectories were run for about 3×10^5 iterations. The phase volume covered by the trajectories was obtained with a precision of 10^{-3}. The accuracy was verified by changing the number of cells, number of iterations, and also by the computation of analytically known phase volumes.

The Poincaré recurrence distribution or the distribution of time of staying in the chamber can be determined in different ways: (i) an initial domain $\Delta\Gamma$ in the phase space can be selected; (ii) the phase space domain $\Delta\Gamma$ can be taken in such

TABLE II. Absolute values for moments of the recurrences distribution function in Figs. 7, 9, and 11.

	S	C	S	C
Moments	No contact		With contact	
1	1.92×10^3	1.97×10^3	1.92×10^3	1.91×10^3
2	7.46×10^6	8.11×10^6	7.49×10^6	7.93×10^6
3	4.42×10^{10}	5.43×10^{10}	5.43×10^{10}	1.02×10^{10}

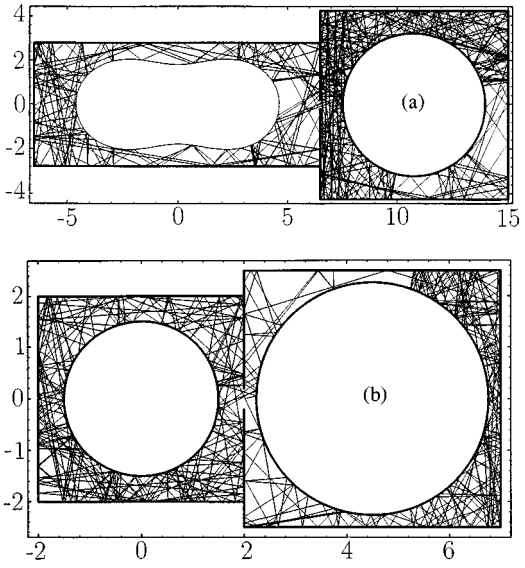

FIG. 13. Two other examples of billiards: (a) *C-S* type; (b) *S-S* type.

a way as to include a part of the billiard's side (for example, the hole); (iii) the domain $\Delta\Gamma$ can be selected to include the entire side y and the entire interval of $v_y \in (-1,1)$. All three cases produced the same distributions $P(t)$. This is a strong confirmation of good accuracy of computations.

We also consider the distributions $P_S(t)$, $P_C(t)$ for three hole sizes (0.1, 0.2, and 0.4) to verify the independence of the normalized distributions on the hole size, and we also consider the case of two equal contacting Sinai billiards to determine the existence of equilibrium.

VIII. OTHER EXAMPLES AND DISCUSSIONS

Two other examples were considered in the same way as the case described above. One example corresponds to the contact between a Cassini and a Sinai billiard [Fig. 13(a)], and another to the contact between two nonequal Sinai billiards [Fig. 13(b)]. The results were the same as above; i.e., there were no equal distributions or moments even for extremely long computations with times longer than 10^{10}. In particular, the distribution of the staying time for left and right chambers of the nonequal *S-S* contacted billiards is presented in Fig. 14(a) and the corresponding moments are presented in Fig. 14(b). Although the phase volumes are equal, the difference in geometry leads to a difference in the distribution functions. In the absence of powerlike tails, one can expect a relaxation to the equilibrium distribution after a certain time interval. This has not happened in the considered cases, even for two different contacted Sinai billiards because their tails of distribution functions produce extremely long-lived fluctuations that do not dissipate in a finite time.

The models of the connected two billiards considered in this paper are very demonstrative and fairly easy to simulate. At the same time, these processes have a fairly long time of crossover to the tails of the Poincaré recurrence distribution because freely bouncing ballistic trajectories do not induce a

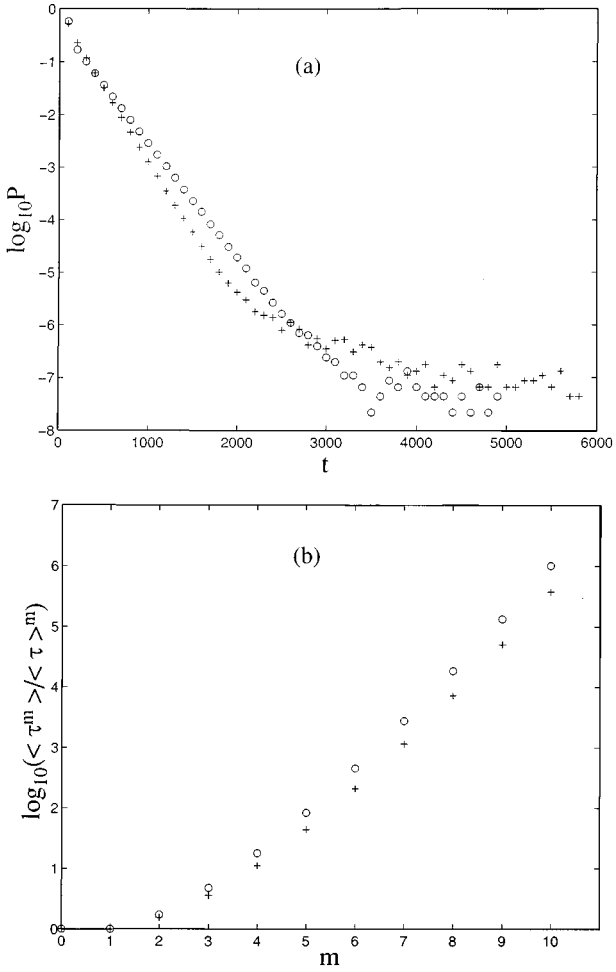

FIG. 14. Results for the *S-S* billiard as in Fig. 13(b): (a) the same as in Fig. 10 but with circles for the right box and crosses for the left box; (b) the moments as in Figs. 11, 12.

strong singularity in the phase space. One can assume the presence in the phase space of a singular zone related to the accelerator mode [6,28]. Therefore, one could get different samples of the distribution function depending on where and how far from the singular zone the domain of observation is taken. The difference, of course, will dissipate with time but the time required exceeds any reasonable value and cannot be included in any physical consideration. Hence there is a need for another type of thermodynamics, which would include a possibility of long lasting fluctuations. The described dynamical model of the Maxwell's Demon works because the equilibrium conditions cannot be formulated on the basis of the canonical laws of thermodynamics.

ACKNOWLEDGMENTS

We want to express our gratitude to V. Afraimovich, L. Bunimovich, J. Goodman, Y. Pesin, M. Shlesinger, and Y. Sinai for numerous valuable discussions. This work was supported by the U.S. Department of the Navy, Grant No. N00014-93-1-0218 and by the U.S. Department of Energy, Grant No. DE-FG02-92ER54184.

[1] *Maxwell's Demon*, edited by H. S. Leff and A. Rex (Princeton University Press, Princeton, NJ, 1990).
[2] G. M. Zaslavsky, Chaos **5**, 653 (1995).
[3] I. C. Percival, in *Nonlinear Dynamics and the Beam-Beam Interaction*, edited by M. Month and J. C. Kerrera, American Institute of Physics Conf. Proc. Vol. 57 (AIP, New York, 1979), p. 302; S. Aubry, in *Solitons and Condensed Matter Physics*, edited by A. R. Bishop and T. Shneider (Springer-Verlag, New York, 1978), p. 264.
[4] J. D. Meiss and E. Ott, Physica D **20**, 387 (1986).
[5] V. Melnikov, in *Transport, Chaos, and Plasma Physics 2*, edited by S. Benkadda, F. Doveil, and Y. Elskens (World Scientific, Singapore, 1996), p. 142.
[6] G. M. Zaslavsky, M. Edelman, and B. Niyazov, Chaos **7**, 159 (1997).
[7] J. D. Meiss, Phys. Rev. A **34**, 2375 (1986); Rev. Mod. Phys. **64**, 795 (1992).
[8] J. D. Meiss, Physica D **74**, 254 (1994).
[9] M. F. Shlesinger, G. M. Zaslavsky, and J. Klafter, Nature (London) **363**, 31 (1993).
[10] G. M. Zaslavsky, Physica D **76**, 110 (1994); Chaos **4**, 25 (1994).
[11] E. W. Montroll and M. F. Shlesinger, in *Studies in Statistical Mechanics*, edited by J. Lebowitz and E. Montroll (North-Holland, Amsterdam, 1984), Vol. 11, p. 1; M. F. Shlesinger, Physica D **38**, 304 (1989).
[12] M. F. Shlesinger, Annu. Rev. Phys. Chem. **39**, 269 (1988).
[13] V. Afraimovich, Chaos **7**, 12 (1997).
[14] V. Afraimovich and G. M. Zaslavsky, Phys. Rev. E. **55**, 5418 (1997).
[15] N. S. Krylov, *Works on the Foundation of Statistical Physics* (Academy of Sciences, Leningrad, 1950) (English translation: Princeton University Press, Princeton, NJ, 1979).
[16] Y. G. Sinai, Dokl. Akad. Nauk SSSR **153**, 1261 (1963) [Sov. Math. **4**, 1818 (1963)].
[17] L. A. Bunimovich and Y. G. Sinai, Math. USSR-Sb. **90**, 407 (1973); Commun. Math. Phys. **78**, 479 (1981).
[18] Y. G. Sinai, Usp. Mat. Nauk. **25**, 141 (1970).
[19] B. V. Chirikov and D. L. Shepelyansky, Physica D **13**, 394 (1984).
[20] W. Bauer and G. F. Betsch, Phys. Rev. Lett. **65**, 2213 (1990).
[21] O. Legrand and D. Sornette, Physica D **44**, 229 (1990).
[22] G. M. Zaslavsky and M. Tippett, Phys. Rev. Lett. **67**, 3251 (1991).
[23] G. M. Zaslavsky, *Chaos in Dynamical Systems* (Harwood Academic, New York, 1985).
[24] P. M. Bleher, J. Stat. Phys. **66**, 315 (1992).
[25] R. Artuso, G. Casati, and I. Guarneri, Phys. Rev. E **51**, R3807 (1995); J. Stat. Phys. **83**, 145 (1996).
[26] P. Dahlquist and R. Artuso (unpublished).
[27] V. V. Afanasiev, R. Z. Sagdeev, and G. M. Zaslavsky, Chaos **1**, 143 (1991).
[28] G. M. Zaslavsky and B. Niyazov, Phys. Rep. **283**, 73 (1997).
[29] S. Benkadda, S. Kassibrakis, R. White, and G. Zaslavsky, Phys. Rev. E **55**, 4909 (1997).
[30] L. A. Bunimovich, Y. G. Sinai, and N. I. Chernov, Russ. Math. Surv. **46**, 47 (1991).
[31] J.-P. Bouchaud and P. Le Doussal, J. Stat. Phys. **41**, 225 (1984).
[32] J. Machta, J. Stat. Phys. **32**, 555 (1983); J. Machta and B. Reinhold, *ibid.* **42**, 949 (1986); J. Machta and R. Zwanzig, Phys. Rev. Lett. **48**, 1959 (1983).
[33] B. Friedman and R. F. Martin, Jr., Phys. Lett. **105A**, 23 (1984).
[34] A. Zacherl, T. Geisel, and J. Nierwetberg, Phys. Lett. **114A**, 317 (1986).
[35] M. Kac, *Probability and Related Topics in Physical Sciences*, Boulder, Colorado, 1957 (Wiley Interscience, New York, 1958).
[36] Y. G. Sinai, *Topics in Ergodic Theory* (Princeton University Press, Princeton, NJ, 1994).
[37] J. D. Meiss, Chaos **7**, 39 (1997).